Proceedings of the Seventh International Conference on
Railway Technology: Research, Development and Maintenance
Edited by: J. Pombo
Civil-Comp Conferences, Volume 15, Paper 17.10
Civil-Comp Press, Edinburgh, United Kingdom, 2026
ISSN: 2753-3239, doi: 10.4203/ccc.15.17.10

Track Geometry Reconstruction Applying the Unknown Input Observer Algorithm

**V. M. Mahieu, M. Santelia, I. La Paglia,
E. Di Gialleonardo, S. Alfi and A. Facchinetti**

Department of Mechanical Engineering, Politecnico di Milano, Italy

Abstract

This paper proposes a model-based approach for the estimation of railway track irregularities, based on the implementation of an Unknown Input Observer (UIO). A multibody railway vehicle model developed in Simpack is used to simulate acceleration signals measured by sensors installed on the bogies and carbody during regular operation. The analysis considers a vehicle travelling at different constant speeds, representative of typical metro line conditions, on both straight and curved tracks. The objective is to reconstruct key track irregularities, namely vertical alignment and cross level, using onboard measurements, and to assess the performance of the proposed identification algorithm. To this end, several evaluation metrics are introduced, showing a good agreement between actual and reconstructed track profiles. The results demonstrate that the proposed approach is effective for track irregularity identification and suitable for monitoring applications based on instrumented in-service vehicles.

Keywords: railway infrastructure, condition-based maintenance, in-service vehicle, model-based solution, rail vehicle dynamic simulation.

1 Introduction

Track geometry is routinely monitored using dedicated Track Recording Vehicles (TRVs) equipped with specialized measurement systems. Although highly accurate measurements can be obtained, TRVs are costly and can interfere with normal operations, motivating the development of alternative approaches based on inertial sensors installed on in-service trains. These approaches aim to infer track geometry from the dynamic response of the vehicle [1]. Unlike TRV-based inspections, this procedure does not require interrupting regular service or restricting measurements to limited time windows (typically during nighttime), thereby reducing operational disruptions and enabling continuous track monitoring, with the potential to detect defects at an early stage.

Once measurement data are collected from in-service vehicles, different processing strategies can be adopted, broadly classified into data-driven and model-based approaches. In the former, relatively simple techniques, such as double integration of acceleration signals, are commonly used [2]. More advanced signal processing methods have also been explored, including spectral analysis, band-pass filtering, and wavelet transforms, to isolate different track geometry components [3-4]. In contrast, model-based approaches rely on mathematical or numerical representations of the vehicle to describe the relationship between measured responses and excitation inputs [5]. These methods typically address an inverse problem, reconstructing track geometry from measured data through observer-based algorithms. Among these, the Kalman filter is widely used, modelling track irregularities as stochastic processes [6-7]. Within the model-based framework, the Unknown Input Observer (UIO) represents an alternative approach. The UIO is designed to decouple and reconstruct unknown inputs directly from measured outputs, without requiring statistical assumptions on the excitation signals. This methodology has previously been applied to track geometry reconstruction for vehicles operating at constant speed [8-9], successfully estimating vertical alignment on both straight and curved tracks using simplified vehicle models.

In this work, the focus shifts to lower vehicle speeds, representative of metro line operations. In addition to vertical alignment, the reconstruction of cross-level irregularities is also addressed. The wavelength range of interest is the D1 range (3-25 m), which is commonly used for infrastructure safety assessment [10]. Furthermore, the performance of the UIO is evaluated under more realistic operating conditions, including low-speed regimes, measurement noise, and multiple excitation sources.

2 Theoretical Background on UIO algorithm

The Unknown Input Observer (UIO) is a model-based estimation technique designed to reconstruct the system state while remaining robust to a class of unknown inputs. Its key feature lies in the ability to decouple the effect of these disturbances from the observer dynamics through an appropriate structural design. As a result, a UIO can provide accurate state estimates even when part of the system input is not measured. Furthermore, and most importantly for the purposes of this work, the estimation of the unknown input naturally arises as a by-product of the observer formulation.

In the present work, track irregularities are treated as unknown inputs acting on the vehicle system through the wheel-rail contact. The objective is to reconstruct these inputs by exploiting measurements of the vehicle dynamic response and applying the UIO framework to infer the underlying track geometry.

To this end, consider the following state-space representation of a continuous-time linear system affected by unknown inputs (time dependence is omitted for brevity):

$$\begin{aligned} \dot{x} &= A\,x + B\,u + E\,d \\ y &= C\,x \end{aligned} \tag{1}$$

where $x \in \mathbb{R}^n$ denotes the state vector, $u \in \mathbb{R}^r$ the known input vector, $y \in \mathbb{R}^m$ the output measurements, and finally $d \in \mathbb{R}^r$ the unknown input vector. A, B, C and E are matrices of suitable dimensions, associated with the system, input, output and disturbances respectively. For the given system, a classical Luenberger observer would take the following form [11]:

$$\begin{aligned} \dot{\hat{x}} &= A\,\hat{x} + B\,u + L(y - \hat{y}) \\ \hat{y} &= C\,\hat{x} \end{aligned} \tag{2}$$

where L is the user-defined observer gain matrix. Additionally, an observer is known as a UIO if the estimation error, defined as follows:

$$e = x - \hat{x} \tag{3}$$

converges to zero asymptotically, and the error e is independent from the disturbance d [12]. Manipulating the Equations (1)-(3), it is possible to derive the dynamic evolution of the estimator error as:

$$\dot{e} = (A - LC)\,e + E\,d \tag{4}$$

which shows that, for classical Luenberger observer, the disturbance d feeds directly through the matrix E in the estimation of the error.
In this framework, Figure 1 illustrates the UIO structure through a block diagram. The observer introduces an additional observer state $z \in \mathbb{R}^n$ defined as:

$$\begin{aligned} \dot{z} &= F\,z + TB\,u + K\,y \\ \hat{x} &= z + H\,y \end{aligned} \tag{5}$$

where new matrices F, T, K and H are suitably defined matrices. In order to decouple the effect of the disturbance d from the estimation error dynamics, the following conditions must be satisfied:

$$\begin{aligned} 0 &= (I - HC)\,E & T &= I - HC \\ F &= TA - K_1 C & K_2 &= FH \end{aligned} \tag{6}$$

with $K = K_1 + K_2$.
The resulting estimation error dynamics can be written as:

$$\dot{e} = Fe = (TA - K_1 C)\,e \tag{7}$$

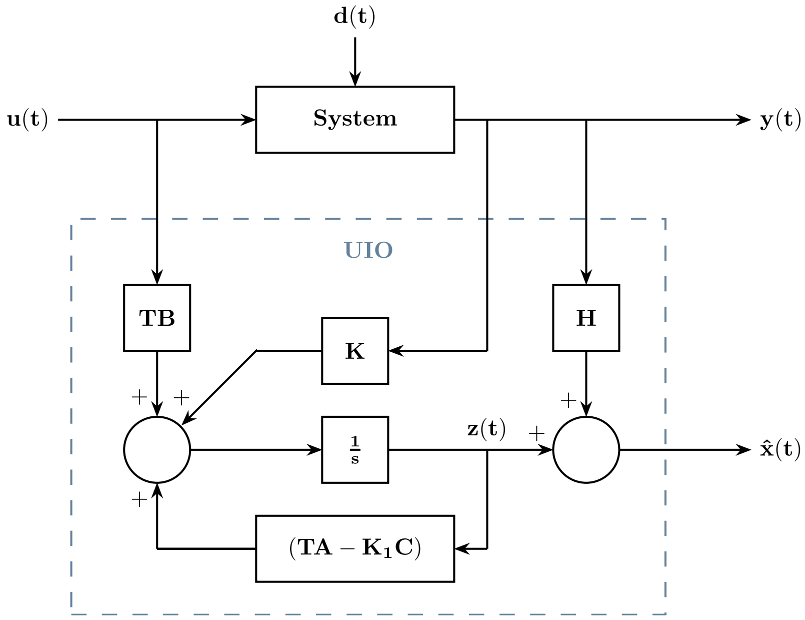

Figure 1 - Block scheme for the implementation of the UIO algorithm.

It is worth noting that Equation (7) does not contain any feedthrough of the disturbance term d. By comparing Equation (7) with the Luenberger structure in Equation (4), it is evident that, in the UIO algorithm, TA acts as the system matrix, while K_1 represents the observer gain. Therefore, by properly tuning K_1, stable eigenvalues can be found for F, ensuring that the estimation error e asymptotically converges to zero.

For a proper design of the UIO, two conditions must be satisfied:

1. $rank(CE) = rank(E)$
2. (C, A_1) is a detectable pair, where $A_1 = (I - HC)A = TA$

The first condition implies that CE has full column rank. The second condition ensures detectability of the pair (C, A_1), which is assessed in this work through a finite-horizon approximation of the observability Gramian. Once these conditions are verified, the observer gain K_1 is tuned such that the estimation error matrix F is stable. This allows the estimation of the states of the system adopting Equation (5). However, the primary objective of this work is not state estimation itself, but rather the reconstruction of the unknown input acting on the system. This quantity can be obtained as a by-product of the observer formulation as follows:

$$\hat{d} = (CE)^+(\dot{y} - CA\,\hat{x} - CB\,u) \tag{8}$$

where $(\quad)^+$ denotes the left pseudoinverse operation.
It is also worth noting that Equation (8) requires not only the knowledge of the state estimate $\hat{x}$, but also the output derivative $\dot{y}$, as will be discussed in the application of the UIO to the identification of railway track irregularity.

3 Application of UIO to track irregularity reconstruction

In this work, the methodology proposed in [8-9] is extended. Previous studied demonstrated the feasibility of reconstructing vertical track irregularities using a 6 degree-of-freedom (DOF) vehicle model within the UIO framework.

3.1 Linear vehicle model

Since the focus of this study is on the reconstruction of both vertical alignment and cross level irregularities, the vehicle model has been extended to a 9-DOF linear system. This model captures the vertical, roll and pitch motions of the rigid bodies, namely the carbody, and the front and rear bogies. The reference vehicle is a typical metro vehicle. A schematic representation of the adopted model is shown in Figure 2. The primary suspensions consist of four spring-damper elements arranged in parallel per each bogie, acting only in the vertical direction. The secondary suspensions adopts a similar configuration with spring-damper elements acting in the vertical, lateral and longitudinal (not reported in Figure 2) directions.

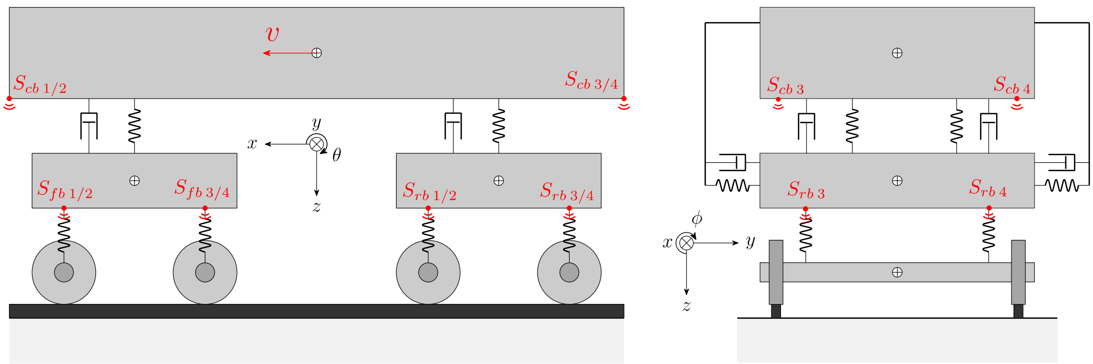

Figure 2: 9-DOF vehicle model considered for the track geometry reconstruction.

3.2 State space formulation

The dynamic model of the vehicle is expressed in state-space form starting from Eq. (1), assuming $u = 0$, i.e., no known input contribution. The system degrees of freedom are arranged as:

$$x_{dof} = \left[z_{fb}\ \theta_{fb}\ \phi_{fb}\ z_{rb}\ \theta_{rb}\ \phi_{rb}\ z_c\ \theta_c\ \phi_c\right]^T \tag{9}$$

where the subscripts fb, rb and c denote the front bogie, rear bogie, and carbody, respectively. Accordingly, the state vector can be written as $x = [x_{dof};\ \dot{x}_{dof}] \in \mathbb{R}^{18}$. Each wheelset is subject to vertical and roll excitations. Therefore, the disturbance vector $\bar{d}$ can be expressed as:

$$\bar{d} = \left[d_{fz1}\ d_{f\phi1}\ d_{rz1}\ d_{r\phi1}\ d_{fz2}\ d_{f\phi2}\ d_{rz2}\ d_{r\phi2}\right]^T \tag{10}$$

where the subscripts f and r refer to the front and rear bogies, respectively. The component z represents the mean vertical alignment excitation, while ϕ denotes the roll excitation induced by cross-level irregularities. The indices 1 and 2 identify the front and rear wheelsets. The disturbance vector is then defined as:

$$d = [\bar{d};\ \dot{\bar{d}}] \in \mathbb{R}^{16} \tag{11}$$

As currently formulated, the problem is not infeasible in principle, since the system includes 18 states and 16 unknown input components. However, a direct application of the UIO would require the reconstruction of a large number of disturbance channels, leading to an unnecessarily complex observer design.

A more convenient formulation can be obtained by exploiting the physical relationship between the excitations acting on the wheelsets. In particular, the disturbances at the rear wheelset of each bogie can be regarded as delayed versions of those acting on the front wheelset, with a time delay determined by the vehicle speed v and the bogie wheelbase l_w, as follows:

$$d_2(t) = d_1(t-\tau), \quad \tau = \frac{2l_{w2}}{v} \tag{12}$$

Based on these system characteristics, two model augmentation strategies are introduced.

First, a second-order Padé approximation is used to model the delay between the excitations d_2 and $\dot{d}_2$ acting on the front and rear wheelset of each bogie. This allows the number of independent disturbances to be reduce to those acting on the front wheelsets only, such that $d_1 \in \mathbb{R}^4$, and $\dot{d}_1 \in \mathbb{R}^4$.

Accordingly, an augmented state vector can be defined as $\tilde{x} = \begin{bmatrix} x \\ x_p \end{bmatrix} \in \mathbb{R}^{34}$, where $x_p \in \mathbb{R}^{16}$ represents the Padè state vector. The dimension of x_p arises from the second-order Padé approximation adopted to model the delay affecting each disturbance component. In particular, each delayed disturbance is described by two states, and considering two trailing wheelsets, two excitation components (vertical displacement and roll), and their derivatives, this results in a total of 16 Padé states. This first augmentation, accounting for the time delay, significantly reduces the number of independent disturbances to be reconstructed.

Furthermore, although d_1 and $\dot{d}_1$ are treated as independent quantities, they are intrinsically related through a differentiation operator. To account for this relationship and further reduce the number of unknown inputs, a second augmentation is introduced by including the disturbance vector d_1 directly in the state. The resulting augmented state vector becomes $x^* = \begin{bmatrix} \tilde{x} \\ d_1 \end{bmatrix} \in \mathbb{R}^{38}$.

As a result of these two augmentation steps, the system dynamics are described by 38 states and 4 unknown input derivatives. Consequently, the quantities of interest can then be obtained by integration.

3.3 Verification of UIO conditions and observer gain

To capture the relevant vehicle dynamics, twelve vertical accelerometers are considered: eight are installed on the bogies (at the primary suspension locations),

with four sensors per bogie, and four are placed at the carbody corners. The measured accelerations are integrated to obtain the observer output y, corresponding to velocities, while the original acceleration signals provide $\dot{y}$.
With reference to the UIO conditions introduced in Section 2, the first condition is satisfied by the selected sensor configuration, as $rank(CE) = rank(E)$. The second condition, namely the detectability of the pair (C, A_1), with $A_1 = TA$, is assessed through a finite-horizon approximation of the observability Gramian, following the approach proposed in [13]. For the considered 9-DOF model, corresponding to a 38-state system, 18 states are found to be detectable. Finally, the observer gain is designed using a Linear Quadratic Estimation (LQE) approach.

4 Results

Once the implementation details of the UIO for track geometry reconstruction have been established, the focus shifts to the analysis of the reconstruction performance. To generate the measurements required by the observer, a detailed multibody model of the metro vehicle is developed in the commercial software Simpack. As described in Section 3.1, the vehicle consists of a single carbody supported by two bogies, connected through secondary suspensions and linked to the wheelsets via primary suspensions.
Regarding the operating conditions, vertical, cross-level, and lateral track excitations are introduced in the Simpack model based on the power spectral density defined in ERRI B176 for vertical and roll components (large defects [14]). The wavelength content is set within the range $\lambda \in [1,70]$ m, corresponding to an extension of the D1 and D2 wavelength bands specified by the standard [10].
To emulate measurement signals collected by onboard sensors, noise is added to the simulated accelerations obtained from Simpack simulations. In particular, reference is made to commercially available MEMS sensors. Low-noise devices with noise densities of 0.01 and 0.20 $\mathrm{mg_{rms}}/\sqrt{\mathrm{Hz}}$ were considered for carbody and bogie accelerometers, respectively [8]. The noisy signals are generated assuming a Gaussian noise distribution with a cutoff frequency of $f_c = 100$ Hz, according to:

$$y = \tilde{y} + n \frac{noise_{density} \sqrt{f_c}}{rms(n)} \tag{13}$$

where $\tilde{y}$ denotes the simulated acceleration measured at the carbody or bogie, and n is a zero-mean Gaussian noise signal.

4.1 Performance metrics

To evaluate the reconstruction quality, both the spatial- and frequency-domain analyses are considered. The spatial-domain analysis provides insight into how accurately the track profile is reconstructed along the track, while the frequency-domain analysis assesses the ability to capture different wavelength components over the entire track section. For brevity, only two spatial-domain metrics are presented in the following.

- Rolling RMSE (rRMSE): starting from the definition of the Root Mean Square Error (RMSE), this metric is computed over a rolling window of length 25 m, consistent with the D1 wavelength band under analysis:

$$rRMSE(x) = \sqrt{\sum_{i=-n}^{n-1} \frac{\left(\hat{y}(x + i\Delta x) - y(x + i\Delta x)\right)^2}{2n}} \tag{14}$$

- Rolling PCC (rPCC): the Pearson Correlation Coefficient (PCC) measures the linear correlation between two signals independently of their amplitude. It ranges between ± 1 corresponding to perfect positive or negative correlation, and 0, indicating no correlation. Using the same 25 m rolling window, it is defined as:

$$rPCC(x) = \frac{\sum_{i=-n}^{n-1}\left(\hat{y}(x + i\Delta x) - \hat{\mu}(x)\right)\left(y(x + i\Delta x) - \mu(x)\right)}{\sqrt{\sum_{i=-n}^{n-1}\left(\hat{y}(x + i\Delta x) - \hat{\mu}(x)\right)^2}\sqrt{\sum_{i=-n}^{n-1}\left(y(x + i\Delta x) - \mu(x)\right)^2}} \tag{15}$$

4.2 Track geometry reconstruction

Different operating scenarios are considered to investigate the influence of vehicle speed and track characteristics on the reconstruction quality. In particular, simulations are performed on straight tracks at two constant speeds (10 and 45 km/h), as well as on a S-shaped curved track consisting of two consecutive curves with a radius of 150 m, at a speed of 45 km/h.

As a first application of the UIO algorithm, Figure 3 presents the results obtained for a vehicle travelling at 10 km/h along a straight track section 800 m long. Figure 3a) and 3d) show the comparison between the reference excitations (shown in blue), and the reconstructed profiles (shown in red), for vertical alignment and cross level, respectively. The reconstructed profiles are obtained from noisy measurement signals. To assess the performance of the proposed algorithm, the metrics introduced in Section 4.1 are also reported: Figures 3b and 3c show the rRMSE and the rPCC for the vertical alignment reconstruction, while Figures 3e) and 3f) show the corresponding metrics for cross-level identification. For completeness, the metrics obtained under noise-free conditions are also included. These are not shown in Figures 3a) and 3d) for clarity, as the differences are negligible.

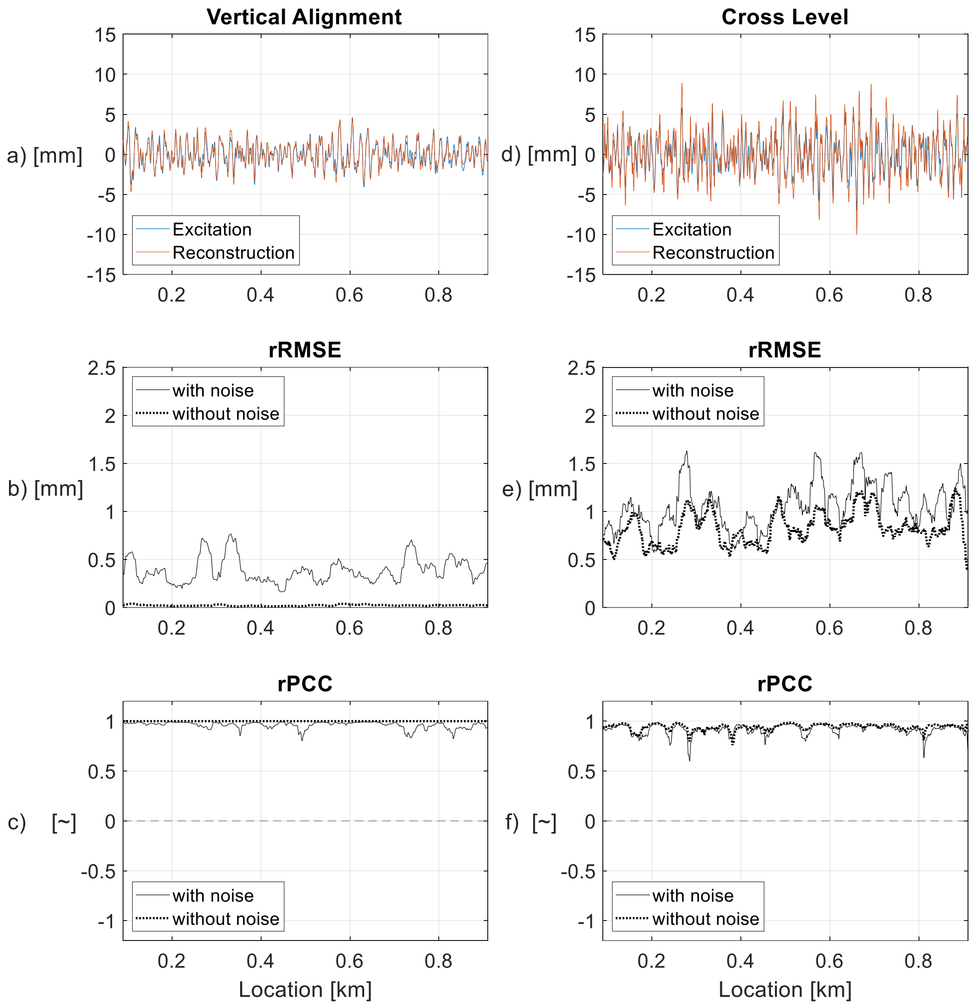

Figure 3: Reconstructions of vertical alignment and cross level, straight track simulation at constant speed of 10 km/h, given measurement noise.

Analysing the metrics reported in Figure 3, satisfactory reconstruction performance is achieved for both track geometry components. However, the presence of measurement noise leads to a slight degradation in the identification accuracy.

More specifically, for vertical alignment, the reconstruction is nearly ideal under noise-free conditions, as indicated by the rRMSE values approaching 0 mm (Figure 3b)) and the rPCC values approaching one (Figure 3c)). When noise is introduced, the performance deteriorates, and discrepancies become visible in the reconstructed profiles shown in Figure 3a). In contrast, the reconstruction of the cross-level component is inherently less accurate, even under noise-free conditions. This is reflected in the deviations from ideal values observed in Figures 3e) and 3f). As expected, the presence of noise further degrades the reconstruction quality.

In the second scenario analysed, the vehicle travels at 45 km/h along the same straight track. The corresponding reconstruction results are presented in Figure 4, using the same representation as in Figure 3.

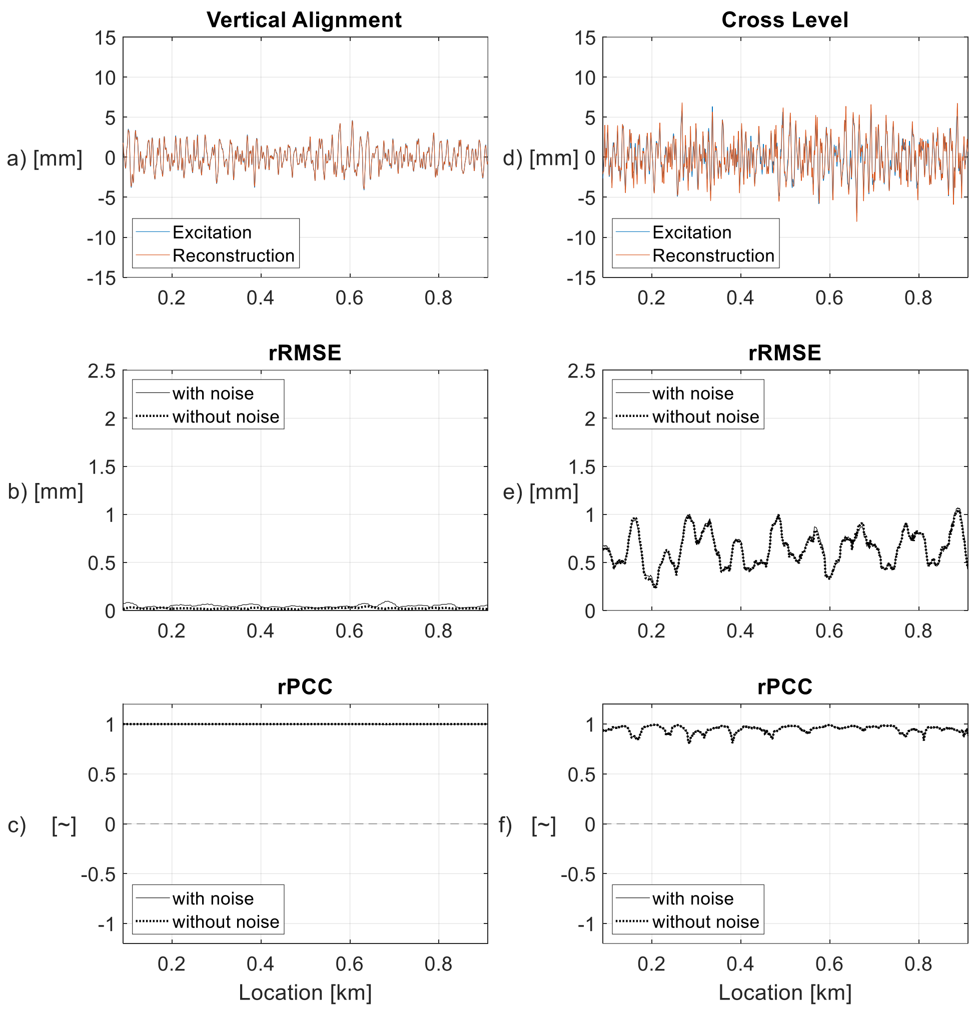

Figure 4: Reconstructions of vertical alignment and cross level, straight track simulation at constant speed of 45 km/h.

Interestingly, Figure 4 shows that the reconstruction quality improves as the vehicle speed increases. An overall enhancement of the performance metrics can be observed compared to the lower-speed case presented in Figure 3. In particular, the rRMSE approaches 0 mm in Figure 4b) and remains below approximately 1 mm for the cross-level component (Figure 4e)). Similar improvements are observed in the rPCC values (Figures 4c) and 4f)) which approach unity more closely than in the 10 km/h scenario. Furthermore, the impact of measurement noise becomes less significant at higher speeds. This is evident from the metrics reported in Figure 4, where the results obtained with and without noise solid and dotted lines) are nearly indistinguishable. This behaviour can be explained by the fact that the measured quantities are accelerations (and their integrals, i.e., velocities), whose amplitude tends to increase with the vehicle speed. As a result, the dynamic response of the vehicle becomes more pronounced, leading to an improved signal-to-noise ratio and, consequently, better reconstruction performance.

As a final example of the algorithm application, an S-shaped track is considered, consisting of two consecutive curves with opposite directions, each with a radius of 135 m, connected by a straight section. The vehicle speed is set to 45 km/h.

It is observed that the same conclusions regarding the effect of measurement noise hold also for curved track conditions. Therefore, only results obtained from noisy measurements are presented in Figure 5, as they represent a more realistic scenario for onboard sensing. The same representation used in the previous figures is adopted, with the addition of the track curvature in the last row (Figures 5d) and 5h)).

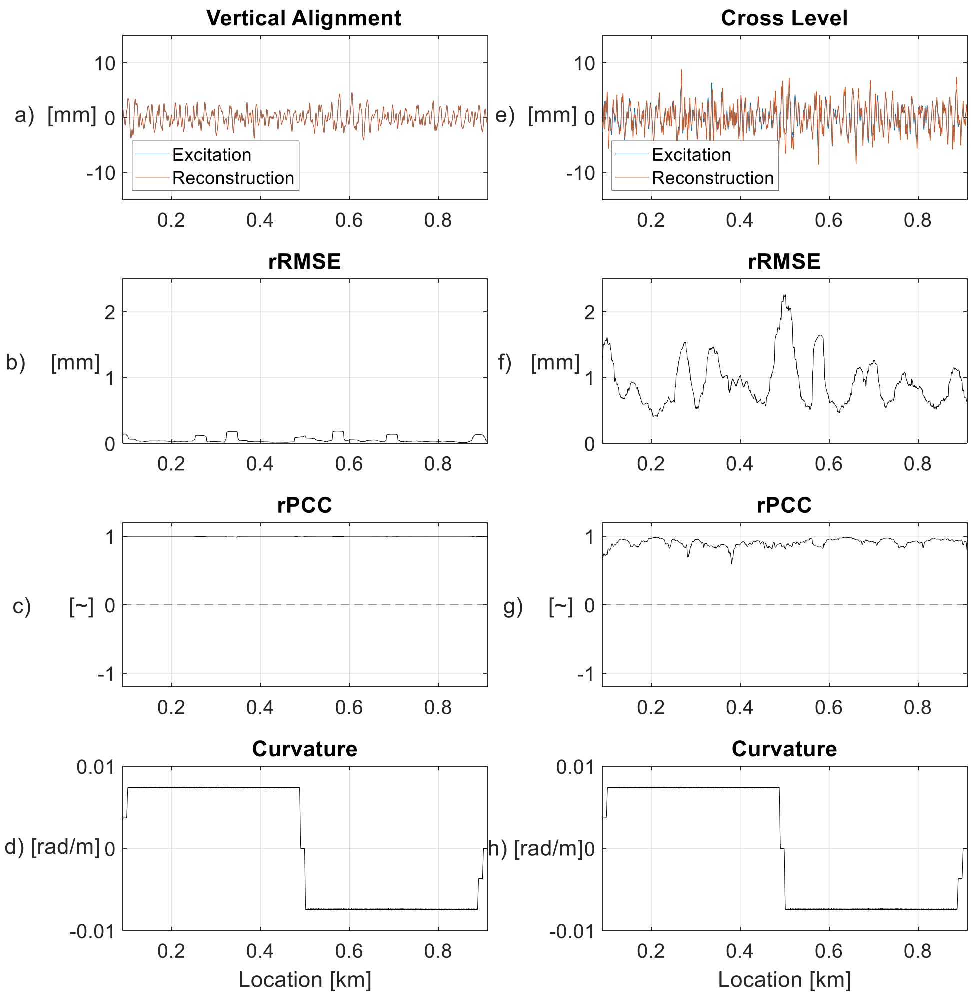

Figure 5: Reconstructions of vertical alignment and cross level, curved track simulation at constant speed of 45 km/h.

As a general observation, Figure 5 shows that satisfactory reconstruction results can also be achieved for curved track sections. In particular, very accurate reconstruction of vertical alignment is obtained (Figures 5a) – 5c)), with performance comparable to that observed on straight track at the same vehicle speed.
In contrast, the identification of the cross-level component is less accurate compared to the tangent track case (Figures 5e) – 5g)(. In particular, variations in track curvature lead to a degradation of the rRMSE, as shown in Figure 5f). This effect is especially evident in the centre of the section, where the vehicle transitions from a right-hand curve to a left-hand curve.
This behaviour can be explained by the additional roll dynamics induced by curve negotiation, which introduce components in the vehicle response that are not directly related to cross-level irregularities. As a result, the observer faces greater difficulty in isolating the contribution of the track geometry from the overall system response.
On the other hand, the rPCC metric (Figure 5g)) appears to be less sensitive to curvature variations.

5 Conclusions and Contributions

In this paper, an Unknown Input Observer (UIO) algorithm has been applied to reconstruct two key railway track irregularity components, namely vertical alignment and cross level, within the 3-25 m wavelength range. The measurement data required by the algorithm have been generated through simulations performed in the multibody software Simpack, using a detailed model of a metro vehicle.
Different operating scenarios have been investigated, including both straight and curved tracks, with the vehicle travelling at medium-to-low speeds. Acceleration measurements from the carbody and bogies have been used as input to the UIO algorithm, with sensor noise included to emulate realistic operating conditions.
The reconstruction performance has been evaluated by comparing the reference track irregularities with the estimated profiles, as well as through quantitative metrics based on rolling RMSE and PCC computed over 25 m windows, consistent with the wavelength range of interest. The results show satisfactory agreement, particularly for vertical alignment, across all analysed speeds. For cross-level irregularities, the reconstruction accuracy improves with increasing vehicle speed.
Overall, the results demonstrate that the proposed approach is effective for track irregularity identification and shows strong potential for condition monitoring applications based on instrumented in-service vehicles.

References

[1] P. Weston, C. Roberts, G. Yeo, E. Stewart, "Perspective on railway track geometry condition monitoring from in-service railway vehicles", Veh. Syst. Dyn., 53, 7, 1063-1091, 2015, DOI:10.1080/00423114.2015.1034730
[2] P. F. Weston, C. S. Ling, C. Roberts, C. J. Goodman, P. Li, R. M. Goodall, "Monitoring vertical track irregularity from in-service railway vehicle", Proc. Inst. Mech. Eng. Part F J. Rail Rapid Transit, 221, 75-88, 2007, DOI:10.1243/0954409JRRT65

[3] H. Tsunashima, Y. Naganuma, T. Kobayashi, “Track Geometry Estimation from Car-Body Vibration”, Veh. Syst. Dyn. 2014, 52, 207–219.

[4] M. Bocciolone, A. Caprioli, A. Cigada, A. Collina, “A Measurement System for Quick Rail Inspection and Effective Track Maintenance Strategy”. Mech. Syst. Signal Process. 2007, 21, 1242–1254

[5] Ding, S.X. Model-Based Fault Diagnosis Techniques: Design Schemes, Algorithms and Tools; Advances in Industrial Control; Springer: London, UK, 2013; ISBN 978-1-4471-4798-5

[6] A. De Rosa, S. Alfi, S. Bruni, “Estimation of lateral and cross alignment in a railway track based on vehicle dynamics measurements”. Mech Syst Signal Process 2019; 116: 606–623, DOI: 10.1016/j.ymssp.2018.06.041

[7] A. De Rosa, R. Kulkarni, A. Qazizadeh, et al., “Monitoring of lateral and cross level track geometry irregularities through onboard vehicle dynamics measurements using machine learning classification algorithms”. Proc. Inst. Mech. Eng. Part F J. Rail Rapid Transit 2021; 235(1): 107–120. DOI: 10.1177/0954409720906649

[8] S. Alfi, M. Santelia, I. La Paglia, E. Di Gialleonardo, A. Facchinetti, “Identification of Railway Vertical Track Alignment via the Unknown Input Observer”, Applied Sciences, 15, 11332,https://doi.org/10.3390/app152111332

[9] I. La Paglia, M. Santelia, S. Alfi, E. Di Gialleonardo, A. Facchinetti, “An Application of the Unknown Input Observer Algorithm for the Identification of Vertical Railway Track Irregularity”; Proceedings of the 6th International Conference on Railway Technology – Railways 2024, Prague, Czech Republic, 1-5 September 2024; doi:10.4203/ccc.7.19.5

[10] EN 13848-5:2017; Railway Applications—Track—Track Geometry Quality. Part 5: Geometry Quality Levels—Plain Line, Switches and Crossings. European Standard: Brussels, Belgium, 2017.

[11] Luenberger, D. An Introduction to Observers. IEEE Trans. Autom. Control. 1971, 16, 596–602

[12] C. Commault, J-M. Dion, O. Sename, R. Motyeian, “Unknown input observer-A structural approach”. In 2001 European Control Conference (ECC), pages 888–893, September 2001.

[13] B. Moore, “Principal component analysis in linear systems: Controllability, observability, and model reduction”. IEEE Transactions on Automatic Control, 26(1):17–32, February 1981

[14] UIC. ORE Power Spectral Density of Track Irregularities. In Part 1: Definitions, Conventions and Available Data; Question ORE C116-Rp1 1971; UIC Railway Publications: Paris, France, 1971